

Electric-Field-Assisted Electron Transfer in a Porphine–Quinone Complex: A Theoretical Study

Pekka J. Aittala,** Oana Cramariuc, and Terttu I. Hukka*

Department of Chemistry and Bioengineering, Tampere University of Technology, P.O. Box 541, 33101 Tampere, Finland, Department of Physics, Tampere University of Technology, P.O. Box 692, 33101 Tampere, Finland, and IT Center for Science and Technology, Av. Radu Beller 25, Bucharest, Romania

Received July 7, 2009

Abstract: The effects of a static external electric field on the ground state electronic structure of a porphine–quinone (PQ) complex have been studied by using density functional theory (DFT). The energies of the excited states have been calculated with time-dependent density functional theory (TDDFT) and with the approximate coupled cluster singles and doubles (CC2) method. The geometries of porphine and quinone have been optimized with B3LYP. The influence of the external electric field on the PQ complex has been studied at six different intermolecular distances between 2.5 and 5.0 Å with the BH&HLYP functional. An external electric field clearly affects the orbitals localized mostly on quinone but not the orbitals localized on porphine. Additionally, the effect of the external field increases with the increasing intermolecular distance. The optical absorption spectrum of porphine obtained by using the BH&HLYP functional is consistent with the Gouterman model and with the spectrum previously calculated with CAM-B3LYP. The potential energy curves of the Q and B states and the lowest charge transfer (CT) states of the PQ complex calculated by using the BH&HLYP with TDDFT functional have also been compared with those obtained with the CC2 method. Both methods show that the lowest CT state is clearly above the Q states when no external field is applied. Therefore, when the Q states of a porphine–quinone system are excited, the conical intersection is not possible and cannot thus provide a path for electron transfer (ET). The calculations show that the Q and B states are affected by the field much less than the lowest CT state. Consequently, the calculations show that the CT state crosses the Q and B states at certain field strengths. Thus, it is possible that the external electric field triggers ET in porphine–quinone systems via conical intersection.

1. Introduction

Electron transfer (ET) plays a crucial role in the photosynthesis taking place in a reaction center. The initial step of photosynthesis is the photoexcitation of the light-harvesting chlorophyll, which forms a so-called special pair with a neighboring quinone, the whole system being embedded in protein. Once chlorophyll is photoexcited, an electron is

transferred from chlorophyll to quinone. This initial ET in the special pair is a starting point of several subsequent electron transfer reactions in the reaction center.¹ The initial efficient ET step has attracted special attention over the years as scientists have tried to establish the mechanism of the ET reaction. Staab and co-workers^{2–4} have synthesized relatively simple model systems for studying the first reaction step of photosynthesis composed of porphyrin derivatives linked covalently with cyclophane bridges to quinone for studying the photoinduced ET. They have found out that, when the porphyrin moiety of the zincporphyrin–quinone donor–acceptor dyads is photoexcited into the energetically

* Corresponding author tel.: +358(0)331153636; e-mail: pekka.aittala@tut.fi.

† Department of Chemistry and Bioengineering.

‡ Department of Physics.

§ IT Center for Science and Technology.

lowest excited state (the Q state), its fluorescence is quenched on a picosecond timescale. This implies efficient electron transfer from the porphyrin to the quinone, which has also turned out to be insensitive for the solvent environment.³ On the contrary, in dyads consisting of a free-base porphyrin (porphine) and quinone, the fluorescence lifetime is strongly dependent on the polarity of the surrounding solvent. In polar solvents, the lifetime is on the same order of magnitude as in dyads consisting of zincporphyrin, but in nonpolar hexane the fluorescence lifetime is almost 10 ns, which is comparable to the lifetime of an unquenched porphine. Therefore, it has been concluded that there is no ET taking place from porphine to quinone in nonpolar solvents.²

Also, in several theoretical studies, ET from porphine derivatives to quinone has been investigated.^{5–8} Worth and Cederbaum have studied the potential energy curves of the B, Q, and CT states of a zincporphyrin–quinone complex along the intermolecular distance by using the CIS method. They concluded that the CT states are in the same energy region with the B states localized on zincporphyrin. Additionally, the energies of the CT states depend more strongly on the molecular geometry than those of the local porphyrin states. Therefore, the CT states are likely to cross the B states, and these crossing points are part of a conical interaction seam proposed as a mechanism of formation of the CT state.⁵ Worth and Cederbaum continued their work with Dreuw and Head-Gordon by studying a covalently linked zincporphyrin–quinone dyad by using time-dependent density functional theory (TDDFT) combined with Δ DFT/CIS. Their calculations showed that two large-scale motions, the “swinging-bridge” and the “twist motion” of the quinone moiety with respect to porphyrin, may cause excited state crossings between the locally excited Q states and the porphyrin-to-quinone CT state. Thus, these motions can trigger ultrafast ET from zincporphyrin to quinone via conical intersection, which is a region of coordinate space where two potential energy surfaces meet with a certain topology.⁶

Zheng et al. applied the INDO/S method to compute the electronic couplings via the two-state generalized Mulliken–Hush (GMH) approach of π -stacked porphyrin–bridge–quinone systems. The phenyl linkers were found to dominate the mediation of the donor–acceptor coupling and the relatively weak exponential decay of the rate with distance aroused from the compression of the π -electron stack.⁷ Olaso-González et al. studied the chlorin–quinone complex using CASPT2 and CASSCF methods. They concluded that ultrafast ET in a chlorin–quinone complex is possible only if the relative orientation of the donor and acceptor molecules allows some overlap of the LUMOs of the molecules. They agreed with Worth et al.⁶ that large-scale motions must take place in the photosynthetic reaction centers to fulfill the observed ultrafast ET.⁸

The surrounding environment usually has a significant influence on the molecular properties. For example, an electric field induced by ambient molecules, for example, by zeolites and peptides, is reported to affect the molecular geometry, molecular orbital distribution, and dipole moments.⁹ Furthermore, high electric fields (up to 10^9 V/m) induced by the large dipole moments of peptides are

proposed to affect the electron transfer taking place between a donor and an acceptor embedded in between parallel peptide chains.¹⁰ In some theoretical studies, the effects induced by an external electric field on molecular and electronic properties have been investigated. These studies have been focusing both on single molecules^{9,11–14} and on donor–acceptor dyads.^{15,16} However, cofacial dyads and complexes have not been much studied theoretically under the influence of an external electric field.¹⁷

Density functional theory (DFT) has been established as an efficient and reliable method for studying the ground state properties of molecules and solid systems. Furthermore, TDDFT has proven to be a reliable and facile method for calculating the properties of excited states.¹⁸ However, the exchange–correlation functionals used currently in TDDFT calculations are reported to suffer from some well-documented shortcomings. In particular, TDDFT is known to underestimate the long-range CT excitations. This so-called CT failure of TDDFT is a consequence of the local nature of both the local density (LDA) and gradient corrected (GGA) approximations to the exact energy functional, which do not contain the derivative discontinuities required by the exact exchange–correlation potential.^{18,19} Inclusion of a fraction of nonlocal Hartree–Fock exchange has been shown to improve results, as exemplified by the use of the “half and half” functional BH&HLYP (BHandHLYP) in the investigation of several excitations with CT character.^{20–22}

In the current study, we have used DFT and TDDFT to investigate the effect of the electric field, which can be also induced by ambient molecules, on the excited state properties of a cofacial porphine–quinone^{3,4} (PQ) donor–acceptor complex by simulating the surrounding effects with a static external electric field. The molecular structure of the studied complex is presented in Figure 1. We have used the hybrid BH&HLYP functional, which incorporates a high fraction (50%) of HF exchange. For example, in the case of a chlorin derivative bacteriochlorophyll *b*, this functional has been reported to yield a rather good excitation spectrum.²³ However, as the BH&HLYP is not expected to completely remedy the CT failure of TDDFT, we have complemented our study by employing also the approximate coupled cluster singles and doubles (CC2) method. The SV(P) basis set, which is roughly identical to 6-31G*, has been used in all density functional calculations. The 6-31G* basis set has been previously successfully applied to calculations of the excited states of an isolated porphine¹⁵ and a zincporphyrin–quinone dyad.⁶ In CC2 calculations, we have used the TZVP basis set, which has been reported to be adequate for CC calculations of low-lying excited states not having Rydberg character.²⁴

The aim of this study has been two-fold. First, we have studied the performance of the BH&HLYP functional in calculating the optical absorption spectrum of porphine because the current GGA functionals and hybrid functionals with a low fraction of Hartree–Fock (HF) exchange have been reported to yield qualitatively incorrect spectra for porphyrins and chlorophylls.¹⁵ The second and the more important aim has been to study the effect of an electric field

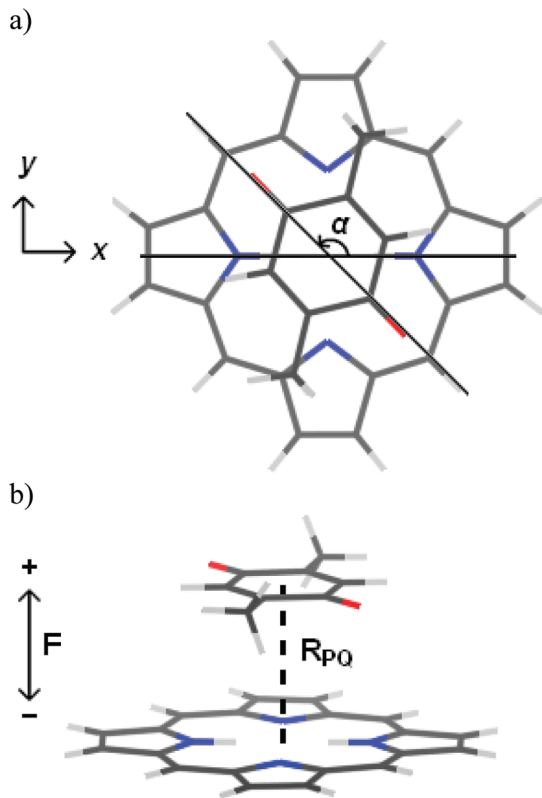


Figure 1. (a) Top view of a porphine–quinone complex. The rotation angle α is the angle between the axes drawn through the two oxygens of quinone and through the two “center” hydrogens of porphine. (b) Side view of the complex. R_{PQ} is the distance between the geometric center points of porphine and quinone. The external electric field (F) has been applied in the direction of a positive (+) or negative (–) z axis, that is, perpendicular to porphine and quinone planes. The direction of the external electrostatic field has been defined as a direction of the movement of a positive charge.

aligned perpendicularly to the porphine and quinone planes on the electronic properties of a PQ complex.

2. Computational Methods

The ground state geometries and the single-point energies were calculated by using DFT.^{25,26} In geometry optimizations, Becke’s three-parameter hybrid functional (B3LYP)^{27–32} was applied, whereas in the single-point energy calculations, the “half-and-half” hybrid functional BH&HLYP^{27–30,33} (BHandHLYP) was used. The BHandHLYP functional consists of 0.5(LDA + B88) + 0.5HF exchange and LYP correlation functionals. In all DFT calculations, the Karlsruhe split valence basis set with one set of polarization functions for all atoms except for hydrogen (SV(P))³⁴ was applied.

Vertical excitation energies were calculated with TDDFT^{35–37} by using the BHandHLYP functional. Only the singlet states were considered. The computed transitions were transformed into simulated absorption spectra by applying a uniform Gaussian broadening with a standard deviation of 0.1 eV. The TDDFT-calculated excitation energies were compared to the energies calculated with the approximate coupled cluster singles and doubles (CC2)³⁸ method, employed in the RICC2 module^{39–41} in Turbomole. In the CC2

Table 1. Rotation Angles α (deg),^a Optimized Intermolecular Distances R_{PQ} (Å), and the Relative Energies E (kJ/mol) of A–H Calculated at the DFT/B3LYP/SV(P) Level of Theory

conformer	α	R_{PQ}	E
A	0	4.01	1.6
B	15	4.05	2.2
C	45	3.89	1.8
D	60	3.93	2.6
E	90	3.92	3.2
F	110	3.92	2.6
G	120	3.85	1.3
H	135	3.82	0

^a See Figure 1a for definition.

calculations, the frozen-core approximation was employed for the 1s orbitals of the carbon and nitrogen atoms. In the excited state calculations, the SV(P) and TZVP³⁴ basis sets were applied, and in the CC2 calculations, an auxiliary basis set⁴² of the same quality was used.

The order of the magnitude of the strength of the external electric field (10^9 V/m) considered in this study corresponds to the electric field observed in peptides, zeolites, and protein cavities. Additionally, we have studied fields of 1×10^9 V/m, 2×10^9 V/m, and 4×10^9 V/m. In the calculations including external electric field, the field (F) was applied in the direction of a positive (+) or negative (–) z axis, that is, perpendicularly to the porphine and quinone planes, see Figure 1 b. The direction of the external electrostatic field was defined as a direction of the movement of a positive charge. All calculations presented in this study were performed with the Turbomole 5.9–5.10 software packages.⁴³

3. Results

3.1. Ground State Energies and Geometries. First, the geometries of quinone and porphine were optimized. Second, the two molecules were superimposed so that porphine was set on the xy plane by setting its geometric center point to the origin, and the z axis was directed through the geometric center point of quinone. Eight conformers (A–H) were made by rotating the quinone with respect to the z axis, that is, by changing the rotation angle α , see Figure 1a for the details. In all conformers, the intermolecular distance (R_{PQ}) was set to 2.5 Å. Thereafter, the conformers were optimized at the DFT/B3LYP/SV(P) level.

Rotation angles α , optimized intermolecular distances, and the relative energies are presented in Table 1. The absolute energies are given in Table S2 in the Supporting Information. In the lowest-energy conformer (H) presented in Figure 1b, the two methyl groups of quinone are almost on the top of the two free nitrogens of porphine, and the two hydrogens of quinone are almost on the top of the center hydrogens of porphine. The structural characteristics of conformer H are given in Table S1 in the Supporting Information. The energies of conformers A–H differ by 3.2 kJ/mol, at the most. A slight distortion from the lowest-energy geometry induces only a small change in energy, see the energies of G and H. The optimized intermolecular distance (R_{opt}) of the lowest-energy conformer H was found to be 3.82 Å at

Table 2. Complexation Energies (kJ/mol) of the PQ Complexes with Intermolecular Distances R_{PQ} (Å) of 2.5, 3.0, 3.5, 4.0, 4.5, and 5.0 Å Calculated under the Influence of an External Electric Field F of -4 , -2 , -1 , 0 , $+1$, $+2$, and $+4 \times 10^9$ V/m at the BH&HLYP/SV(P)//B3LYP/SV(P) Level of Theory

F	R_{PQ}					
	2.5	3.0	3.5	4.0	4.5	5.0
-4	305.9	11.6	-7.2	-5.7	-1.6	0.2
-2	301.7	9.1	-9.2	-7.2	-2.7	-0.8
-1	299.3	7.6	-10.4	-8.1	-3.5	-1.4
0	296.5	5.8	-11.8	-9.1	-4.3	-2.0
$+1$	293.5	3.9	-13.3	-10.2	-5.1	-2.7
$+2$	290.3	1.7	-15.0	-11.5	-6.1	-3.4
$+4$	282.8	-3.3	-19.0	-14.5	-8.3	-5.1

the B3LYP/SV(P) level, and further calculations with BH&HLYP yielded 3.60 Å.

In the current study, one of the aims is to investigate the effect of the intermolecular distance R_{PQ} on the electronic properties of a porphine–quinone complex. Therefore, six conformers were made from the most stable PQ complex H in the following way. The optimized geometries of porphine and quinone were kept frozen, and the R_{PQ} was set to 2.5, 3.0, 3.5, 4.0, 4.5, and 5.0 Å. The complexes are denoted as PQ_{2.5}, PQ_{3.0}, PQ_{3.5}, PQ_{4.0}, PQ_{4.5}, and PQ_{5.0}, respectively. Single-point energy calculations were carried out at the BH&HLYP/SV(P) level of theory for these structures.

Complexation energy, which indicates the stability of the complex, was calculated as the difference between the sum of the isolated porphine and quinone and the energy of the interacting PQ complex. Table 2 summarizes the complexation energies of the PQ_{2.5}, PQ_{3.0}, PQ_{3.5}, PQ_{4.0}, PQ_{4.5}, and PQ_{5.0} complexes calculated under the influence of an external electric field of $+4$, $+2$, $+1$, 0 , -1 , -2 , and -4×10^9 V/m. The orientation of the external electric field has been defined in section 2. Without the presence of the external field, the PQ complexes with $R_{PQ} \geq 3.5$ Å have negative complexation energies. The absolute value of the complexation energy of PQ_{3.5}, PQ_{4.0}, and PQ_{4.5} exceeds the thermal energy at room temperature (~ 2.48 kJ/mol), and porphine and quinone are therefore bound together in these complexes. The PQ_{2.5}, PQ_{3.0}, and PQ_{5.0} would not exist without linkers because the thermal fluctuation would dissociate the complexes. It is also noteworthy that the single-point energy calculations predict the minimum of complexation energy to be 3.5 Å, that is, close to R_{opt} (3.6 Å). This implies that the geometries of porphine and quinone are not much affected by the complexation. The DFT does not, however, take into account the van der Waals interactions, and calculations at the CC2/TZVP level indicate much more stable complexes with complexation energies of $+13.4$, -123.9 , -97.7 , -60.4 , -35.4 , and -20.7 kJ/mol for PQ_{2.5}, PQ_{3.0}, PQ_{3.5}, PQ_{4.0}, PQ_{4.5}, and PQ_{5.0}, respectively. Hence, the CC2 calculations predict a minimum in the ground state potential energy curve (PEC) at a shorter R_{PQ} than DFT, and the minimum is also much steeper than the rather flat PEC obtained with DFT (see also Figure 5).

The complexation energies increase when the external field increases, see Table 2. Additionally, the external field affects

less when the intermolecular distance R_{PQ} increases. When the external electric field increases by 1×10^9 V/m from -4×10^9 V/m to $+4 \times 10^9$ V/m, the complexation energy of PQ_{2.5} increases by 2.1–3.6 kJ/mol. In PQ_{3.0}, PQ_{3.5}, PQ_{4.0}, PQ_{4.5}, and PQ_{5.0}, an increase of the external field by 1×10^9 V/m increases the complexation energy by 1.3–2.5, 1.0–2.0, 0.8–1.5, 0.6–1.1, and 0.5–0.9 kJ/mol, respectively. Therefore, the complexation energies are affected more by the intermolecular distance between the porphine and quinone than by the external electric field.

3.2. Ground State Electronic Structures. *Without the External Electric Field.* The localizations and energies of the molecular orbitals (MOs) reveal the nature of the excited states and provide insight into the absorption spectra of the PQ complexes. Therefore, we will concentrate here on the orbitals that are involved in transitions giving rise to the Q, B, and the lowest CT bands of the PQ complexes, see section 3.3. Additionally, isoamplitude surfaces, orbital energies, as well as variation of the orbital energies in porphine–quinone complexes as a function of the external electric field of the HOMO–2, HOMO–3, HOMO–4, LUMO+3, and LUMO+4 orbitals is provided in the Supporting Information. In order to illustrate the differences in localizations of the MOs, isoamplitude surfaces of HOMO–1, HOMO, LUMO, LUMO+1, and LUMO+2 of PQ_{2.5}, PQ_{3.0}, PQ_{3.5}, PQ_{4.0}, and PQ_{4.5} are presented in Figure 2. Localization of the orbitals of PQ_{5.0} is practically identical to that of the PQ_{4.5} complex, and the isoamplitude surfaces of PQ_{5.0} have been thus omitted. In complexes with short intermolecular distances (PQ_{2.5} and PQ_{3.0}), the interaction of porphine and quinone increases the delocalization of the orbitals. Most of the orbitals of these complexes are delocalized over the whole complex and cannot be clearly related to the orbitals of either the isolated porphine or quinone. However, in PQ_{3.5} the delocalization of the orbitals is decreased, and the orbitals of PQ_{4.0}, PQ_{4.5}, and PQ_{5.0} are almost entirely localized on either porphine or quinone. In these complexes, the electronic structure is roughly the combination of the orbitals of the isolated porphine and quinone.

Comparison of the isoamplitude surfaces of the other complexes with those of PQ_{3.5} reveals that LUMO and LUMO+2 cross, that is, change places, when the intermolecular distance increases to 4.0 Å, see Figures 2 and 3. These orbitals retain their reversed order when the intermolecular distance increases further.

The HOMO and HOMO–1 orbitals of the PQ complexes arise from the degenerate HOMO and HOMO–1 of porphine. The LUMO and LUMO+1 of the PQ_{2.5}, PQ_{3.0}, and PQ_{3.5} complexes and LUMO+1 and LUMO+2 of the PQ_{4.0}, PQ_{4.5}, and PQ_{5.0} complexes arise from the degenerate LUMO and LUMO+1 of the isolated porphine. The LUMO+2 of the PQ_{2.5}, PQ_{3.0}, and PQ_{3.5} complexes and LUMO of the PQ_{4.0}, PQ_{4.5}, and PQ_{5.0} complexes can be related to LUMO of the isolated quinone. The energies of the two highest occupied and three lowest unoccupied molecular orbitals of PQ_{2.5}, PQ_{3.0}, PQ_{3.5}, PQ_{4.0}, PQ_{4.5}, and PQ_{5.0} are presented in Table 3. Additionally, the energies of the corresponding orbitals of the isolated porphine and quinone are shown. The energies of the orbitals localized on porphine in PQ_{3.5} differ

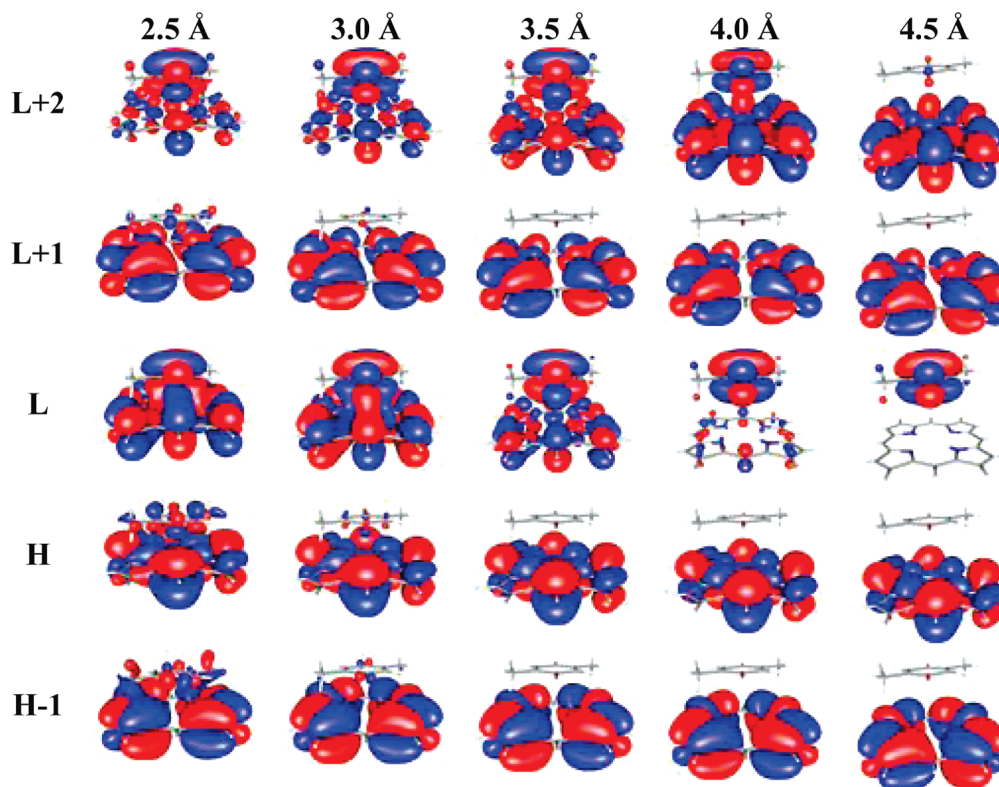


Figure 2. Some of the orbitals of the PQ complexes with intermolecular distances of 2.5, 3.0, 3.5, 4.0, and 4.5 Å calculated at the BH&HLYP/SV(P)//B3LYP/SV(P) level of theory without an external electric field. The isoamplitude surfaces of the orbitals presented are 10% of the maximum positive (red) and minimum negative (blue) amplitudes of the wave functions.

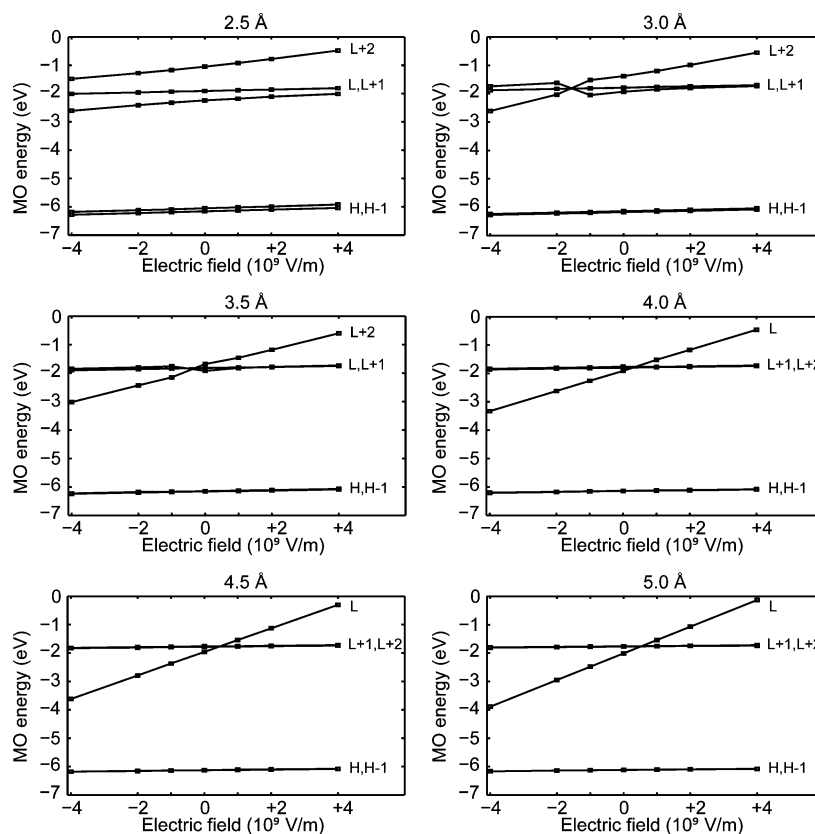


Figure 3. Variation of the orbital energies in porphine–quinone complexes with intermolecular distances of 2.5, 3.0, 3.5, 4.0, 4.5, and 5.0 Å as a function of the external electric field. See Figure 1b for a definition of the direction of the field. Orbitals are labeled according to the PQ complexes in the zero field. The energies are calculated at the BH&HLYP/SV(P)//B3LYP/SV(P) level of theory.

Table 3. Energies (eV) of Some Molecular Orbitals of the PQ Complexes with Intermolecular Distances R_{PQ} (Å) of 2.5, 3.0, 3.5, 4.0, 4.5, and 5.0 Å and the Energies of the Corresponding Orbitals of the Isolated Porphine (P) and Quinone (Q)^a

orbital	R_{PQ}						P	Q
	2.5 Å	3.0 Å	3.5 Å	4.0 Å	4.5 Å	5.0 Å		
LUMO+2	-1.05	-1.38	-1.68	-1.76	-1.76	-1.76	0.32	1.84
LUMO+1	-1.91	-1.79	-1.82	-1.80	-1.78	-1.77	-1.72	0.79
LUMO	-2.24	-1.93	-1.92	-1.91	-1.96	-2.01	-1.74	-2.27
HOMO	-6.05	-6.14	-6.15	-6.14	-6.13	-6.12	-6.08	-9.00
HOMO-1	-6.16	-6.17	-6.16	-6.14	-6.13	-6.12	-6.08	-9.23

^a The energies are calculated at the BH&HLYP/SV(P)//B3LYP/SV(P) level of theory.

only very little (<0.09 eV) from the energies of the corresponding orbitals of the isolated porphine. However, the energies of the orbitals localized entirely on quinone in the PQ complex are ~0.5 eV smaller than the energies of the corresponding orbitals of the isolated quinone.

Changing of the intermolecular distance affects the energies of the MOs in which the isoamplitude surface is either delocalized to both porphine and quinone or localized entirely on quinone (see Figure 2 and Table 3), whereas the energies of the MOs localized on porphine remain practically constant. Except for PQ_{2.5}, the HOMO and HOMO-1 orbitals of the other complexes, localized on porphine, are degenerate, and the energies of these two orbitals do not depend on the intermolecular distance.

The LUMO is delocalized over the whole complex in PQ_{2.5} and PQ_{3.0} and mainly or entirely localized on quinone at $3.5 \leq R_{PQ} \leq 5.0$ Å. The PQ_{2.5} complex has the lowest LUMO energy. At $3.0 \leq R_{PQ} \leq 4.0$ Å, the orbital energy is constant but decreases in PQ_{4.5} and PQ_{5.0} when the interaction between porphine and quinone decreases.

Regardless of the intermolecular distance, the LUMO+1 orbital is entirely localized on porphine, and the energy of the orbital is about the same. At $3.0 \leq R_{PQ} \leq 5.0$ Å, the energy of the orbital changes by 0.08 eV at most.

In PQ_{4.0}, PQ_{4.5}, and PQ_{5.0}, the LUMO+2 orbital is localized mainly on porphine. Thus, the energy of the orbital changes only a little between 4.0 and 5.0 Å. In PQ_{3.5}, PQ_{3.0}, and PQ_{2.5}, the decrease of the intermolecular distance leads to a stronger interaction between porphine and quinone, and the LUMO+2 becomes delocalized over the whole complex. The decrease of the intermolecular distance from 4.0 to 3.5 Å increases the orbital energy by 0.08 eV. When the intermolecular distance is decreased to 3.0 Å and further to 2.5 Å, the energy decreases by 0.30 and 0.33 eV, respectively.

The Effect of the External Electric Field. Variation of the energies of the two highest occupied and three lowest unoccupied MOs of the PQ_{2.5}, PQ_{3.0}, PQ_{3.5}, PQ_{4.0}, PQ_{4.5}, and PQ_{5.0} complexes is presented as a function of the external electric field in Figure 3. Orbitals are labeled in the same way as in the case of the complexes in a zero field. Generally, the effect of the external electric field on the energies of the molecular orbitals delocalized over the whole complex or localized on quinone increases when the intermolecular distance increases.

In PQ_{2.5}, in which porphine and quinone interact strongly, the external electric field affects the orbitals only slightly. Therefore, neither the negative nor the positive electric field induces crossing, that is, no changes in the order of MOs.

The orbital which is more strongly localized on quinone than on porphine, that is, LUMO+2, is affected the most. An increase of the positive electric field strength by 1×10^9 V/m increases the LUMO+2 energy by 0.1–0.16 eV. The negative electric field affects the energies of the LUMO slightly more than the positive field. The increase of the negative field strength by 1×10^9 V/m decreases the orbital energy by ~0.1 eV, whereas the increase of the positive field increases the energy by ~0.06 eV. Every increase of 1×10^9 V/m in the electric field strength increases the energy of the HOMO-1, HOMO, and LUMO+1 orbitals by 0.04 eV at the most.

Evidently, already in the PQ_{3.0} complex, the orbitals localized mainly on porphine and mainly on quinone respond differently to the external electric field. The energy of the LUMO+1 increases by 0.03 eV at the most with an increase of the electric field by 1×10^9 V/m. The LUMO+2 crosses the LUMO when the external field is increased from -1×10^9 to -2×10^9 V/m, see Figure 3. This causes some nonlinear variation in the LUMO energy, but otherwise the energy of the orbital is affected by the external field in the same manner as the LUMO+1 localized on porphine by the external electric stimulation. On the contrary, the LUMO+2 that mostly localizes on quinone is affected much more. Every increase of 1×10^9 V/m in the strength of the electric field increases the energy of the LUMO+2 by ~0.2 eV, but the crossing with LUMO between -1×10^9 and -2×10^9 V/m induces some exceptions to the linear behavior, see Figure 3. Energies of the degenerate HOMO and HOMO-1 are affected in the same way as the energy of the LUMO+1; that is, when the strength of the electric field increases by 1×10^9 V/m, the energy of the HOMO and HOMO-1 increase by 0.03 eV at the most.

In the complexes with longer intermolecular distances (PQ_{3.5}, PQ_{4.0}, PQ_{4.5}, and PQ_{5.0}), the external electric field changes the energies of the orbitals linearly. The energies of the orbitals localized on porphine are only slightly affected by the external field. With a few exceptions, the energies of the degenerate HOMO and HOMO-1 as well as the degenerate LUMO+1 and LUMO+2 (LUMO and LUMO+1 in PQ_{3.5}) increase only by 0.02 eV at the most, with a gradual increase of the strength of the external electric field. Therefore, the energies of the orbitals stay between -6.07 and -6.24 eV, -7.79 and -8.10 eV, and -1.72 and -1.90 eV, respectively (see Figure 3).

On the contrary, the energy of the LUMO (LUMO+2 in PQ_{3.5}) localized more strongly on quinone than on porphine is significantly affected by the external stimulation. Also, in this orbital, a linear dependence between the orbital energy and the external field is observed. The increase in the

Table 4. Energies E (eV) and Oscillator Strengths f of the Q and B Bands of Porphine Calculated with the TDDFT/BH&HLYP, TDDFT/CAM-B3LYP, and CC2 Methods^a

	Q _x		Q _y		B _x		B _y	
	E	f	E	f	E	f	E	f
BH&HLYP/SV(P)	2.27	0.002	2.45	0.002	3.62	0.877	3.76	1.254
BH&HLYP/TZVP	2.25	0.003	2.43	0.003	3.59	0.939	3.69	1.247
CC2/SV(P)	2.30	0.001	2.70	0.003	3.56	0.982	3.65	1.200
CC2/TZVP	2.28		2.67		3.49		3.56	
CC2/SVP ^b	2.32		2.71		3.57		3.66	
CAM-B3LYP/6-31G* ^c	2.2		2.4		3.5		3.6	
experimental ^d	1.98	0.02	2.42	0.07	3.33	1.15	3.33	

^a Experimental values are shown for comparison. ^b Obtained from ref 45. ^c Adopted from ref 15. ^d Obtained from ref 46.

intermolecular distance increases the effect of the external field on the orbital energy, and therefore the lines representing the change of the orbital energy become steeper along with the increasing intermolecular distance. Consequently, the longer the intermolecular distance, the smaller the external electric field that is able to cause the crossing of the orbital localized mostly on quinone with the orbitals localized on porphine.

Because the unoccupied orbitals of the PQ complexes localized on quinone and on porphine respond differently to the external electric field, it is expected that the electric field on the order of magnitude under consideration has a significant influence on the excited states of the PQ complexes. More specifically, the excited states mostly localized on quinone versus on porphine are expected to be influenced by the electric field more than the states localized only on porphine. Therefore, on the basis of the ground state electronic structure, it is expected that the external electric field affects also the electron transfer in the PQ complexes.

3.3. Electronic Absorption Spectra. Porphine. Over 30 years ago, Gouterman presented a four-orbital model⁴⁴ that explained the characteristic Q and B bands of porphines and chlorophylls. The model is widely accepted, but modern TDDFT calculations have shown that one has to go beyond the Gouterman model in order to explain all of the features of the porphine and chlorophyll spectra, for example, also the so-called N states. Among the traditional density functionals, BP86 and B3LYP have been reported as an improvement to the Gouterman model, but it has been recently shown¹⁵ that only the spectra calculated with the computationally demanding CASPT2 method and the recent long-range corrected density functional, that is, CAM-B3LYP, are qualitatively consistent with experiments and support the Gouterman model. The N states, arising from the excitations from orbitals that are localized on two of the pyrrole rings only instead of the whole porphine, have been shown to have CT character. Hence, they respond to an external electric field applied along the porphine plane.¹⁵ The N bands were proven to be significant in porphyrin spectroscopy, but the traditional density functionals underestimate the energies of the N bands clearly. Therefore, it has been concluded that in the TDDFT frame the CAM-B3LYP functional is mandatory for reliable theoretical investigations of the porphine absorption spectra.¹⁵ It can be speculated whether the better performance of CAM-B3LYP compared to the traditional functionals is only due to the larger amount of the HF exchange or because of the range separation which improves

the asymptotic behavior of the exchange potential of the functional. Therefore, we have studied the performance of the BH&HLYP functional, which does not contain the range separation, in calculating the optical absorption spectrum of porphine.

Table 4 summarizes the energies of the Q_x, Q_y, B_x, and B_y bands of porphine calculated by using the TDDFT/BH&HLYP and CC2 methods with the SV(P) and TZVP basis sets. In addition, the energies calculated using CC2/SVP⁴⁵ and TDDFT/CAM-B3LYP/6-31G*¹⁵ are listed for comparison along with the experimental⁴⁶ values. The assignments of the bands were verified by applying a static external electric field of 2×10^9 V/m in the porphine plane, directed along the x and y axes, see Figure 1a. The states shown in Table 4 were not affected by the external field and can thus be confirmed as the Q_x (2.27 eV), Q_y (2.45 eV), B_x (3.62 eV), and B_y (3.76 eV) bands. In contrast, the states lying above the B bands responded to the external stimulation and are thus assigned to the N states. These non-Gouterman states contain mainly excitations from orbitals localized on two of the pyrrole rings only (from HOMO−2 and HOMO−3 to LUMO and LUMO+1).

In agreement with the Gouterman four-orbital model, TDDFT combined with BH&HLYP includes only the HOMO−1, HOMO, LUMO, and LUMO+1 orbitals in the transitions forming the first four excitation bands. Additionally, the energies of the Q and B bands calculated with BH&HLYP are almost identical to those calculated by using the CAM-B3LYP functional.¹⁵ The BH&HLYP functional combined with the SV(P) basis set overestimates the experimental⁴⁶ energies of the Q and B bands by 0.43 eV at most, which is slightly less than the 0.5 eV reported in a study of the bacteriochlorophyll *b*.²³ The BH&HLYP/SV(P) yields the lowest two N states at 3.97 and 4.33 eV, that is, at slightly lower energies than CAM-B3LYP (~4.3 and 4.5 eV). Compared to the results obtained with the SV(P) basis set, the use of the TZVP basis set with BH&HLYP decreases the energies of the Q states by 0.02 eV and those of the B_x and B_y states by 0.03 and 0.07 eV, respectively. Our findings confirm that, although the BH&HLYP functional overestimates the energies of the Q and B bands slightly, the spectrum is qualitatively consistent with the experiments and is in agreement with the results obtained by CAM-B3LYP and CASPT2. Therefore, we conclude that BH&HLYP is also suitable for investigating the properties of porphine derivatives.

The energies of the Q and B bands calculated by using the CC2 method with the SV(P) basis set are equal to the ones reported by Parac and Grimme⁴⁵ and do not differ much from the ones calculated with TDDFT/BH&HLYP/SV(P). Additionally, the two methods yield very similar oscillator strengths for these states. The CC2/SV(P) yields the Q_x and Q_y (2.30 and 2.70 eV) bands at slightly higher energies than TDDFT/BH&HLYP/SV(P), and thus the deviation from the experimental values increase. On the contrary, the CC2/SV(P)-calculated B_x and B_y energies (3.56 and 3.65 eV) are closer to the experimental values than the ones obtained by using TDDFT/BH&HLYP/SV(P). The use of the TZVP basis set instead of SV(P) in the CC2 calculations decreases the energies of the Q_x , Q_y , B_x , and B_y states by 0.02, 0.03, 0.06, and 0.09 eV, respectively.

Porphine–Quinone Complexes. The vertical singlet excitations of the isolated porphine and quinone were compared to the excitations of the $PQ_{2.5}$, $PQ_{3.0}$, $PQ_{3.5}$, $PQ_{4.0}$, $PQ_{4.5}$, and $PQ_{5.0}$ complexes. The simulated absorption spectrum obtained from the TDDFT/BH&HLYP/SV(P) calculations and the corresponding vertical excitations of $PQ_{2.5}$, $PQ_{3.0}$ and $PQ_{3.5}$ are presented in Figure 4a, b, and c, respectively. Except for an additional band, the spectrum of $PQ_{3.5}$ is in principle a superposition of the spectra of the isolated porphine and quinone (not shown). The simulated spectra of the $PQ_{4.0}$, $PQ_{4.5}$, and $PQ_{5.0}$ complexes are almost identical with that of $PQ_{3.5}$, and the assigning of the bands is straightforward. The increasing interaction between porphine and quinone changes the appearance of the spectra slightly in the case of $PQ_{3.0}$. Moreover, in the case of $PQ_{2.5}$, the absorption bands are clearly broader and the intensities of the B bands are smaller, whereas the CT band is more intense than in the spectra of the PQ complexes with longer intermolecular distances. However, in both cases, the identification of the Q, B, and CT states is clear. The use of the TZVP basis set instead of SV(P) affects the energies of the Q, B, and CT bands only very little, and thus the SV(P) basis set is used in the TDDFT calculations of the PQ complexes throughout the rest of this study.

The low-energy excitations at 2.25 eV (HOMO \rightarrow LUMO+1 and HOMO–1 \rightarrow LUMO) and 2.42 eV (HOMO–1 \rightarrow LUMO+1 and HOMO \rightarrow LUMO) in the spectrum of $PQ_{3.5}$ are identified as the Q_x and Q_y bands of porphine, respectively. The excitations with high oscillator strengths at 3.59 eV (HOMO–1 \rightarrow LUMO+1 and HOMO \rightarrow LUMO+2) and 3.67 eV (HOMO \rightarrow LUMO+1 and HOMO–1 \rightarrow LUMO+2) are identified as the Soret band (B_x and B_y , respectively) of porphine. The lowest states, which are localized on quinone, are found at 3.19, 3.47, and 4.00 eV. All excitations between 4.5 and 5 eV are localized porphine states. The band arising from two excitations having energies of 2.83 (HOMO \rightarrow LUMO and HOMO \rightarrow LUMO+2) and 2.90 eV (HOMO–1 \rightarrow LUMO+2 and HOMO–1 \rightarrow LUMO) is not present in the superposition of the simulated spectra of porphine and quinone and can thus be assigned to neither porphine nor quinone. The band is a consequence of the interaction between porphine and quinone and is identified as a porphine-to-quinone CT band.

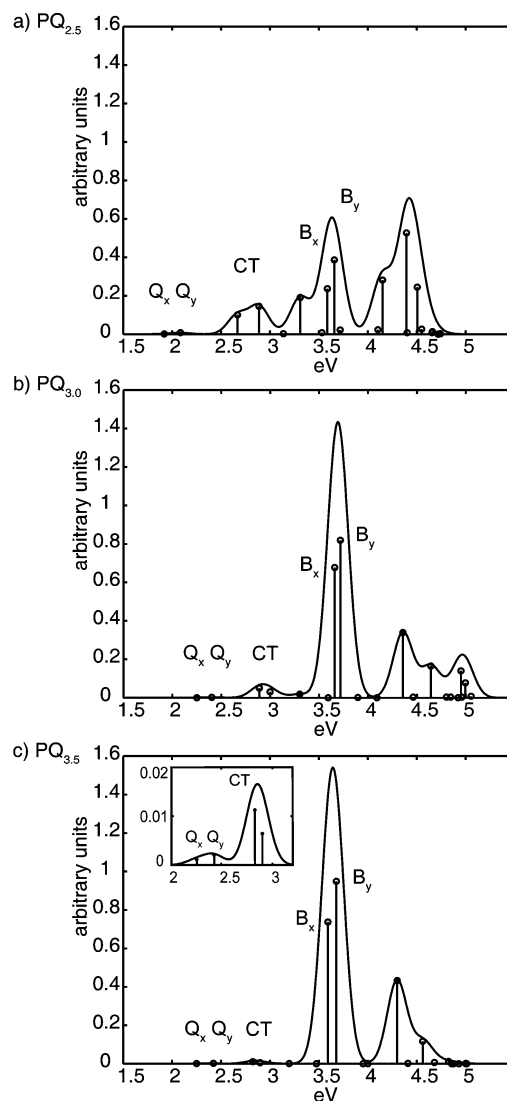


Figure 4. Simulated absorption spectra and the assignments of the Q, B, and CT bands of the PQ complexes with intermolecular distances of (a) 2.5 Å, (b) 3.0 Å, and (c) 3.5 Å calculated without an external electric field at the BH&HLYP/SV(P) level of theory.

3.4. Electron Transfer in Porphine–Quinone Systems.

Recent theoretical studies of the photoinduced ET in zincporphyrin–quinone and in reduced chlorin–quinone systems have shown evidence that conical intersections (CIs) are involved in the underlying mechanism of this process.^{5,6,8} The CIs are regions of coordinate space where two potential energy surfaces meet with a certain topology. Although between two states of the same multiplicity an infinite number of CI points form a crossing seam, the efficient transition from one state to the other occurs usually at the lowest CI. Thus the lowest minimum energy crossing point is of special interest and will constitute a key element in our investigation of the electric-field-mediated ET between porphine and quinone.⁸

In contrast to the zincporphyrin–quinone dyads, the fluorescence lifetime of the Q state of the porphine–quinone dyads² in nonpolar solvents is comparable to that of an unperturbed porphine, thus indicating that there is no ET from porphine to quinone. This would be evidenced by the

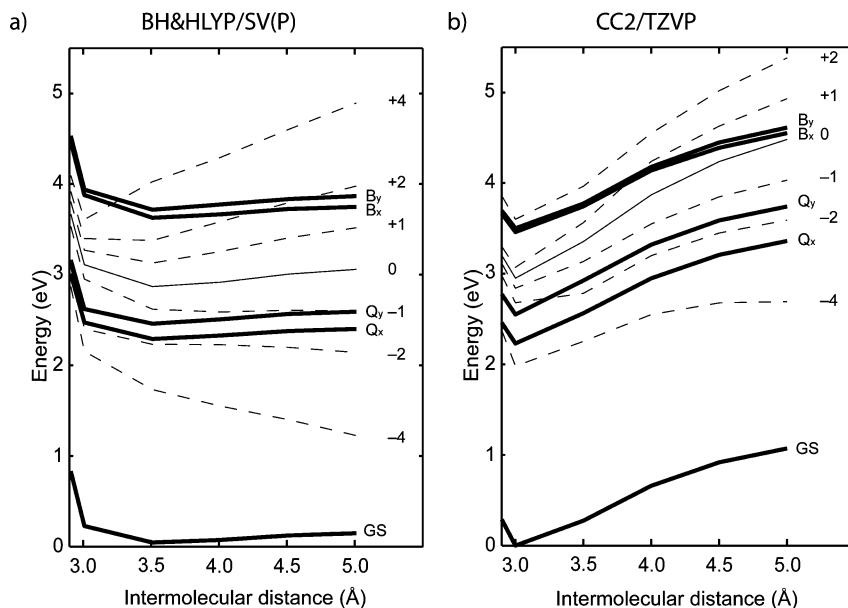


Figure 5. Potential energy curves (PECs) of the ground state (GS); the Q_x , Q_y , B_x , and B_y states (thick solid lines); and the energetically lowest CT state (thin solid line) as a function of the intermolecular distance of the PQ complex calculated without an external electric field. Thin dashed lines represent the PECs of the lowest CT state calculated under the influence of an external electric field of $+4$, $+2$, $+1$, -1 , -2 , and -4×10^9 V/m. The PECs of the Q and B states calculated in the presence of an external field were almost identical to the ones obtained in a zero field (thick solid lines) and have thus been omitted for clarity. The curves of the excited states are plotted relative to the GS curve calculated without the presence of an external field to allow easier comparison. The curves have been calculated at the (a) TDDFT/BH&HLYP/SV(P) and (b) CC2/TZVP levels of theory.

absence of a CI between the potential energy surfaces of the locally excited Q state and that of the CT state. Polar solvents decrease the fluorescence lifetime of porphine–quinone dyads significantly, which indicates that ET from porphine to quinone takes place in polar solvents² and a CI exists between the excited states. Thus, the question that arises is whether an external electric field can induce an ET between porphyrin and quinone in nonpolar solvents, leading to the crossing of the potential energy surfaces of the locally excited porphine states and the lowest CT state.

Without the External Electric Field. The PECs of the ground state; Q_x , Q_y , B_x , B_y states; and the energetically lowest CT state were calculated as a function of the intermolecular distance R_{PQ} of the PQ complex with the TDDFT/BH&HLYP and CC2 methods by applying the SV(P) and TZVP basis sets. The use of the TZVP basis set instead of SV(P) does not affect the energies of the PECs calculated with TDDFT/BH&HLYP. However, if the SV(P) basis set is used with CC2, the lowest CT state crosses the B_x state at $R_{PQ} = 5.0$ Å, but if TZVP is used instead the CT state remains below the B states at the whole R_{PQ} range studied. Hence, the SV(P) basis set can be used in the TDDFT calculations, but in the CC2 calculations the larger TZVP is needed. The PECs calculated at the (a) TDDFT/BH&HLYP/SV(P) and (b) CC2/TZVP levels of theory are presented in Figure 5. The PEC of the lowest CT state calculated with TDDFT/BH&HLYP does not cross either the Q or the B state (Figure 5a), thus indicating that no ET would occur when porphine is locally excited to any of these states. The CC2 calculations yield a similar picture for the Q state (Figure 5b), although the excited state energies are higher than the ones obtained with TDDFT/BH&HLYP. The CC2 method does not predict a crossing between the

CT and B states in the studied R_{PQ} range, either. However, the CT state lies so close to the B states at 5.0 Å that the states could cross at slightly larger distances. Thus, ET from porphine to quinone could be possible, if the B states were excited, which could be a possible process, although this has not been investigated experimentally.

The Effect of the External Electric Field. The PECs of the energetically lowest CT state calculated under the influence of an external electric field of $+4$, $+2$, $+1$, 0 , -1 , -2 , and -4×10^9 V/m are illustrated in Figure 5a and b as thin dashed lines. The curves of the excited states are plotted relative to the ground state curve calculated without the presence of an external field to allow an easier comparison.

Regardless of the direction and the strength, the external electric field does not practically affect the excitation energies of the Q and B states. Therefore, the potential energy curves of these states calculated in the presence of the external field are almost identical to the ones shown in Figure 5 as thick lines, which represent the PEC in the absence of the external field, and have been thus omitted for clarity.

Unlike the energies of the Q and B bands, the energy of the lowest CT band is clearly affected by the external stimulation. A positive orientation of the electric field shifts the energies of the CT state upward toward higher values, while a negative orientation shifts them down. Additionally, the stabilization or destabilization of the CT state is different at different intermolecular distances and depends also on the strength of the electric field. As a consequence, the PECs of CT can be influenced in such a way that they span a range of approximately 3 eV and have different slopes, thus intersecting the PEC of either the Q or the B states (see

Figure 5) at different intermolecular distances. This allows tuning of the electron transfer process as described below.

According to the TDDFT results, with the presence of an external field of $+2 \times 10^9$ V/m, the CT state crosses the B_x and B_y states at an R_{PQ} of ca. 4.3 and 4.7 Å, respectively. This means that under the influence of the positive field the CT state would closely resemble the ground state equilibrium structure, which would favor a fast electron transfer from porphine to quinone. A further increase of the electric field strength to $+4 \times 10^9$ V/m leads to the crossing of the CT and B states already in the inverted region at $q_n R_{PQ}$ of around 3.2–3.3 Å. Negative fields shift the PECs of the CT state further away from the B states and thus clearly hinders the ET if B states are excited. However, the CT state crosses the Q_y state already with the weakest studied negative field at $R_{PQ} \approx 5.0$ Å. The negative field could thus ease the forming of the CT state from the locally excited Q state. There is, however, a threshold after which the increasing of the negative field shifts the crossing of the Q and CT states to the inverted region. When stronger negative fields are applied, the CT crosses both Q states already at $2.5 < R_{PQ} < 3.0$ Å, and the CT state becomes the lowest excited state. Although the general qualitative picture of the influence of the electric field on the CT formation is preserved also by the CC2 calculations, several quantitative conclusions are different.

The external electric field affects the energies of the Q and B states of the PQ complexes calculated by using CC2 (Figure 5b) by about the same amount as the energies calculated by using TDDFT/BH&HLYP. As discussed above, the CC2 calculations reveal that the lowest CT state lies so close to the B states at 5.0 Å that it is likely that the states cross at slightly large distances, when no external field is applied. This means that, if the B states are photoexcited in the zero field, the ET from porphine to quinone could be possible. According to the CC2 calculations, the smallest positive field shifts the crossing of the B states and the CT state to ~ 3.8 Å. An increase of the field to $+2 \times 10^9$ V/m shifts the PEC of the CT state above the B states already at 2.5 Å, and no crossing occurs. In the R_{PQ} of 4.5 and 5.0 Å, the CT state calculated under the influence of $+4 \times 10^9$ V/m lies so much above the B states that the calculation of the CT state energies is not feasible. Thus, the corresponding PEC is totally omitted. However, this PEC is of less importance since it cannot cross the B states. The application of a negative electric field of -1×10^9 V/m decreases the CT state energy such that it lies clearly between the Q and B states, and no state crossings are observed at the intermolecular distances under consideration. When the negative field is increased to -2×10^9 V/m, the energy of the CT state decreases such that the CT state crosses the Q_y state at ca. 3.3 Å. Thus, CT formation from the Q states becomes possible. When the negative field is increased to -4×10^9 V/m, the CT state goes below the Q states already at 2.5 Å, and thus ET is not possible.

Comparison of the Methods. A comparison of our porphine–quinone calculations (TDDFT/BH&HLYP and CC2) with the CIS⁵ and the combined TDDFT/BLYP and Δ DFT/CIS⁶ calculations of the zincporphyrin–quinone

system reveals differences between the two systems and between the performances of the methods. To begin with the locally excited porphine states, the BLYP yields the lowest locally excited quinone state in the zincporphyrin–quinone dyad clearly below the Q states. In our calculations, the lowest local quinone state is clearly above the Q states with an energy almost identical to the energy of the lowest excited state of the isolated quinone. This indicates, as expected, that the interaction is clearly stronger between quinone and zincporphyrin than between quinone and porphine. Moreover, the CIS calculations show that the interaction with quinone breaks the degeneracy of the B states of zincporphyrin, whereas in our CC2 calculations the perturbation of quinone actually increases the degeneracy of the B states of porphine.

Our CC2-calculated PEC of the lowest CT state of the porphine–quinone complex is rather similar to the one that has been calculated for zincporphyrin–quinone by using CIS.⁵ Although the B states calculated with CC2 lie lower in energy than the states predicted by CIS, the CT state lies in both cases just below the B states at 5.0 Å, and it is likely that also in the case of the porphine–quinone complex the states would cross at about 5.5 Å, just like in CIS calculations of the zincporphyrin–quinone complex. A comparison of the CIS calculations with the Δ DFT/CIS calculations carried out by Dreuw and co-workers⁶ reveals that the CIS method overestimates the energies of the CT states of the zincporphyrin–quinone system almost by 2 eVs. However, since porphine is a weaker electron donor than zincporphyrin, the CT states of the porphine–quinone system should lie higher in energy compared to the zincporphyrin–quinone system. Therefore, we expect that the CC2-calculated PEC of the CT state of the PQ complex is not much overestimated.

Comparison between the TDDFT/BH&HLYP and CC2 calculations indicates that both methods predict in principle a similar behavior for the PQ complex under the influence of the external electric field, and only the intermolecular distance, in which the locally excited porphine states (Q and B states) and CT states cross, changes. Considering the quite flat shape of the PEC of the CT state, it is clear that, despite the high fraction of the HF exchange (50%), TDDFT/BH&HLYP underestimates the CT energies at longer intermolecular distances. It could be that the CAM-B3LYP functional,⁴⁷ which has been reported to perform best with parameters that set the HF exchange to 65% in long distances, yields some improvement to the PECs of the lowest CT state. However, currently there is no study in which the performance of BH&HLYP and CAM-B3LYP is compared. The CAM-B3LYP functional has been reported to yield clearly better CT energies than B3LYP,⁴⁷ but also BH&HLYP has been reported to improve the CT calculations as compared to B3LYP.²² On the basis of the porphine spectra calculated with BH&HLYP in this study and with CAM-B3LYP in another study,¹⁵ we expect that the PECs of the Q and B states obtained with these two functionals would be very similar.

Regardless of the method (TDDFT/BH&HLYP or CC2), the calculations show that the CT states of the porphine–quinone complexes can be controlled by an external field

without perturbing the local porphine states. Therefore, an external electric field can be useful in controlling ET in porphine–quinone systems.

5. Conclusions

The influence of a static external electric field on the order of magnitude of 10^9 V/m, corresponding to the magnitude of an electric field induced by large dipole moments of peptides, on the ground state electronic structure and the singlet excited state energies of PQ complexes has been studied by using DFT, TDDFT, and the CC2. Six different intermolecular distances between 2.5 and 5.0 Å have been investigated.

An external electric field affects the energies of the orbitals localized mostly on quinone, whereas the orbitals localized entirely on porphine are hardly affected. Moreover, the effect of the external field on the orbital energies increases when the intermolecular distance increases.

In the current study, we have also shown that BH&HLYP yields a qualitatively correct porphine spectrum in which the N states lie clearly above the Q and B bands. Moreover, the calculated spectrum is almost identical to the one obtained previously by using CAM-B3LYP.

The potential energy curves of the Q and B states and the lowest CT state were calculated as a function of the intermolecular distance of the PQ complex both in the absence and in the presence of an external electric field. Both field directions, that is, from porphine to quinone and from quinone to porphine, were considered. Regardless of the direction or the strength, the external electric field affects the energies of the Q and B states only slightly. On the contrary, the energy of the lowest CT state depends both on the strength and the direction of the external field as well as on the intermolecular distance. Both methods (TDDFT/BH&HLYP and CC2) show that, depending on the strength and direction, the external electric field is able to either induce or hinder crossing of the locally excited porphine states (Q and B) and the lowest CT state. Moreover, crossing can be induced to occur at geometries close to those of the ground state, which would facilitate fast electron transfer. Thus, we conclude that the external electric field can be used to control ET in porphine–quinone systems.

Acknowledgment. Prof. H. Lemmetyinen, the head of the Laboratory of Chemistry at Tampere University of Technology, is acknowledged for offering the facilities for this research. The CSC–IT Center for Science Ltd., governed by the Finnish Ministry of Education, is acknowledged for providing the computing resources. Financing of this research by the Academy of Finland and the Romanian National University Research Council (RP7/6/30.04.2008) is greatly appreciated.

Supporting Information Available: Absolute energies of the complexes A–H and bond lengths and bond angles of the porphine–quinone complex H optimized at the B3LYP/SV(P) and BH&HLYP/SV(P) levels of theory are provided. In addition, isoamplitude surfaces; orbital energies; and a variation of the orbital energies of the HOMO–2, HOMO–3, HOMO–4, LUMO+3, and LUMO+4 orbitals

of the PQ_{2.5}–PQ_{5.0} complexes as a function of the external electric field are provided. This material is available free of charge via the Internet at <http://pubs.acs.org>.

References

- (1) Hoff, A. J.; Deisenhofer, J. *Phys. Rep.* **1997**, *287*, 1–247.
- (2) Heitele, H.; Pöllinger, F.; Häberle, T.; Michel-Beyerle, M. E.; Staab, H. A. *J. Phys. Chem.* **1994**, *98*, 7402–7410.
- (3) Häberle, T.; Hirsch, J.; Pöllinger, F.; Heitele, H.; Michel-Beyerle, M. E.; Anders, C.; Döhling, A.; Krieger, C.; Rückemann, A.; Staab, H. A. *J. Phys. Chem.* **1996**, *100*, 18269–18274.
- (4) Staab, H. A.; Hauck, R.; Popp, B. *Eur. J. Org. Chem.* **1998**, 631–642.
- (5) Worth, G. A.; Cederbaum, L. S. *Chem. Phys. Lett.* **2001**, *338*, 219–223.
- (6) Dreuw, A.; Worth, G. A.; Cederbaum, L. S.; Head-Gordon, M. *J. Phys. Chem. B* **2004**, *108*, 19049–19055.
- (7) Zheng, J.; Kang, Y. K.; Therien, M. J.; Beratan, D. N. *J. Am. Chem. Soc.* **2005**, *127*, 11303–11310.
- (8) Olaso-González, G.; Merchán, M.; Serrano-Andrés, L. *J. Phys. Chem. B* **2006**, *110*, 24734–24739.
- (9) Rai, D.; Joshi, H.; Kulkarni, A. D.; Gejji, S. P.; Pathak, R. K. *J. Phys. Chem. A* **2007**, *111*, 9111–9121.
- (10) Fox, M. A.; Galoppini, E. *J. Am. Chem. Soc.* **1997**, *119*, 5277–5285.
- (11) De Biase, P. M.; Doctorovich, F.; Murdiga, D. H.; Estrin, D. A. *Chem. Phys. Lett.* **2007**, *434*, 121–126.
- (12) Choi, Y. C.; Kim, W. Y.; Park, K. -S.; Tarakeshwar, P.; Kim, K. S.; Kim, T. -S.; Lee, J. Y. *J. Chem. Phys.* **2005**, *122*, 094706–1–094706–6.
- (13) Tsukamoto, S.; Nakayama, T.; Aono, M. *Chem. Phys.* **2007**, *342*, 135–140.
- (14) Ye, Y.; Zhang, M.; Zhao, J. *THEOCHEM* **2007**, *822*, 12–20.
- (15) Cai, Z.-L.; Crossley, M. J.; Reimers, J. R.; Kobayashi, R.; Amos, R. D. *J. Phys. Chem. B* **2006**, *110*, 15624–15632.
- (16) Dahlblom, M. G.; Reimers, J. R. *Mol. Phys.* **2005**, *103*, 1057–1065.
- (17) Fang, Y.; Gao, S.; Yang, X.; Shuai, Z.; Beljonne, D.; Brédas, J. L. *Synth. Met.* **2004**, *141*, 43–49.
- (18) Dreuw, A.; Head-Gordon, M. *Chem. Rev.* **2005**, *105*, 4009–4037.
- (19) Tozer, D. J. *J. Chem. Phys.* **2003**, *119*, 12697–12699.
- (20) Dreuw, A.; Weisman, J. L.; Head-Gordon, M. *J. Chem. Phys.* **2003**, *119*, 2943–2946.
- (21) Liao, M. -S.; Lu, Y.; Scheiner, S. *J. Comput. Chem.* **2003**, *24*, 623–631.
- (22) Magyar, R. J.; Tretiak, S. *J. Chem. Theory Comput.* **2007**, *3*, 976–987.
- (23) Sundholm, D. *Phys. Chem. Chem. Phys.* **2003**, *5*, 4265–4271.
- (24) Schreiber, M.; Silva-Junior, M. R.; Sauer, S. P. A.; Thiel, W. *J. Chem. Phys.* **2008**, *128*, 134110–1–134110–25.
- (25) Treutler, O.; Ahlrichs, R. *J. Chem. Phys.* **1995**, *102*, 346–354.

- (26) Von Arnim, M.; Ahlrichs, R. *J. Comput. Chem.* **1998**, *19*, 1746–1757.
- (27) Dirac, P. A.M. *Proc. R. Soc. London A* **1929**, *123*, 714–733.
- (28) Slater, J. C. *Phys. Rev.* **1951**, *81*, 385–390.
- (29) Becke, A. D. *Phys. Rev. A* **1988**, *38*, 3098–3100.
- (30) Lee, C.; Yang, W.; Parr, R. G. *Phys. Rev. B* **1988**, *37*, 785–789.
- (31) Vosko, S. H.; Wilk, L.; Nusair, M. *Can. J. Phys.* **1980**, *58*, 1200–1211.
- (32) Becke, A. D. *J. Chem. Phys.* **1993**, *98*, 5648–5652.
- (33) Becke, A. D. *J. Chem. Phys.* **1993**, *98*, 1372–1377.
- (34) Schäfer, A.; Horn, H.; Ahlrichs, R. *J. Chem. Phys.* **1992**, *97*, 2571–2577.
- (35) Bauernschmitt, R.; Ahlrichs, R. *Chem. Phys. Lett.* **1996**, *256*, 454–464.
- (36) Bauernschmitt, R.; Häser, M.; Treutler, O.; Ahlrichs, R. *Chem. Phys. Lett.* **1997**, *264*, 573–578.
- (37) Furche, F.; Ahlrichs, R. *J. Chem. Phys.* **2002**, *117*, 7433–7447. Furche, F.; Ahlrichs, R. *J. Chem. Phys.* **2004**, *121*, 12772–12773.
- (38) Christiansen, O.; Koch, H.; Jørgensen, P. *Chem. Phys. Lett.* **1995**, *243*, 409–418.
- (39) Hättig, C.; Weigend, F. *J. Chem. Phys.* **2000**, *113*, 5154–5161.
- (40) Hättig, C.; Hellweg, A.; Köhn, A. *Phys. Chem. Chem. Phys.* **2006**, *8*, 1159–1169.
- (41) Hättig, C.; Köhn, A. *J. Chem. Phys.* **2002**, *117*, 6939–6951.
- (42) Weigend, F.; Häser, M.; Patzelt, H.; Ahlrichs, R. *Chem. Phys. Lett.* **1998**, *294*, 143–152.
- (43) Ahlrichs, R.; Bär, M.; Häser, M.; Horn, H.; Kölmel, C. *Chem. Phys. Lett.* **1989**, *162*, 165–169.
- (44) Gouterman, M.; Wagnière, G. H.; Snyder, L. C. *J. Mol. Spectrosc.* **1963**, *11*, 108–127.
- (45) Parac, M.; Grimme, S. *J. Phys. Chem. A* **2002**, *106*, 6844–6850.
- (46) Edwards, L.; Dolphin, D. H.; Gouterman, M.; Adler, A. D. *J. Mol. Spectrosc.* **1971**, *38*, 16–32.
- (47) Yanai, T.; Tew, D. P.; Handy, N. C. *Chem. Phys. Lett.* **2004**, *393*, 51–57.

CT9003417